DOI: 10.1002/chem.200701691

Switchable Antenna: A Star-Shaped Ruthenium/Osmium Tetranuclear Complex with Azobis(bipyridine) Bridging Ligands

Joe Otsuki,*[a] Arata Imai,[a] Katsuhiko Sato,[a] Dong-Mei Li,[a] Mayumi Hosoda,[a] Masao Owa,[a] Tetsuo Akasaka,[b] Isao Yoshikawa,[b] Koji Araki,[b] Tomoyoshi Suenobu,[c] and Shunichi Fukuzumi*[c]

Abstract: A star-shaped Ru/Os tetranuclear complex, in which a central Os unit is linked to three peripheral Ru units by 4,4′′-azobis(2,2′-bipyridine) (azobpy) bridging ligands, was prepared to examine the unique photodynamics regulated by its redox state. The Ru/Os tetranuclear complex exhibits Ru-based luminescence at 77 K, whereas the three-electron reduction (one for each azobpy) of the Ru/Os complex results in luminescence from the Os unit. The photoexcited state of the Ru/Os complex rapidly decays into low energy metal-to-ligand charge-transfer states, in which the excited electron is localized in the azobpy ligand in the form of azobpy$^{\bullet-}$. Upon the one-electron reduction of the azobpy ligands, the above-mentioned low-energy states become unavailable to the photoexcited complex. As a result, an energy transfer from the Ru-based excited state to the Os-based excited state becomes possible. Ultrafast transient absorption measurements revealed that the energy transfer process consists of two steps; intramolecular electron transfer from the terminal bipyridine ligand (bpy$^{\bullet-}$) to form azobpy^{2-} followed by a metal-to-metal electron transfer. Thus, the Ru/Os tetranuclear complex collects light energy into the central Os unit depending on the redox state of the bridging ligands, qualifying as a switchable antenna.

Keywords: bridging ligands · electron transfer · photochemistry · redox chemistry · time-resolved spectroscopy

Introduction

Manipulating photons and electrons at the molecular or supramolecular level has received considerable attention, as studies on these processes may lay the foundation for the development of molecule-based information processing devices. Electron and energy transfer processes would provide a means for electronic communication among molecular entities in the device. Then, modulation or switching of these processes is required to process information.[1] Alteration of some properties of a control unit in the molecular assembly by external stimuli, such as redox reactions,[2,3] light,[4–7] and chemical species,[8] is used to modulate energy/electron-transfer processes. To widen the scope of molecular switches, it would be important to realize switching in more complex systems than simple on-off switching for a single energy- or electron-transfer process. Recent examples incorporating complex modes of operation include three-way switches,[4a,7a] a molecular re-router,[4c] a T-junction relay,[7b] and a molecular double throw switch.[5b]

We have developed molecular light switches by using homonuclear Ru or Os polypyridine-type complexes that contain 4,4′′-azobis(2,2′-bipyridine)[3a] (azobpy) or 4′,4′′′′-azobis(2,2′:6′,2′′-terpyridine)[3f] (azotpy) as a bridging ligand. When the azo ligand is neutral in these complexes, the metal-to-ligand charge-transfer (MLCT) excited state is rapidly thermally deactivated. As such, these complexes in the as-prepared state are practically non-luminescent. When the azo ligand is one-electron or two-electron reduced, the com-

[a] Prof. J. Otsuki, A. Imai, K. Sato, Dr. D.-M. Li, M. Hosoda, M. Owa
The College of Science and Technology, Nihon University
1-8-14 Kanda Surugadai, Chiyoda-ku, Tokyo 101-8308 (Japan)
Fax: (+81) 3-3259-0817
E-mail: otsuki@chem.cst.nihon-u.ac.jp

[b] Dr. T. Akasaka, Dr. I. Yoshikawa, Prof. Dr. K. Araki
Institute of Industrial Science, University of Tokyo
4-6-1 Komaba, Meguro-ku, Tokyo 153-8505 (Japan)

[c] Dr. T. Suenobu, Prof. Dr. S. Fukuzumi
Department of Material and Life Science
Graduate School of Engineering, Osaka University, SORST
Japan Science and Technology Agency (JST)
2-1 Yamada-oka, Suita, Osaka 565-0871 (Japan)
Fax: (+81) 6-6879-7370
E-mail: fukuzumi@chem.eng.osaka-u.ac.jp

Supporting information for this article is available on the WWW under http://www.chemeurj.org/ or from the author.

plexes behave more or less like the corresponding parent complexes, $[M(bpy)_3]^{2+}$ (M = Ru or Os; bpy = 2,2′-bipyridine) or $[M(tpy)_2]^{2+}$ (tpy = 2,2′:6′,2″-terpyridine). This results in a luminescence emission, characteristic to these kinds of complexes. A homodinuclear Ru complex, $[(bpy)_2Ru(azobpy)\text{-}Ru(bpy)_2]^{4+}$ (**Ru_2**),[3a] and a tetranuclear Ru complex, $[\{(bpy)_2Ru(azobpy)\}_3Ru]^{8+}$ (**Ru_4**), exemplify this class of complexes.[3e]

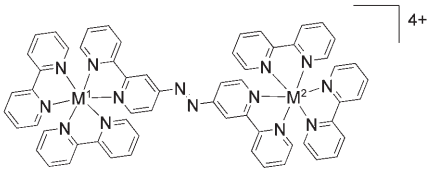

Ru_2: $M^1 = M^2 = Ru$
RuOs: $M^1 = Ru$, $M^2 = Os$
Os_2: $M^1 = M^2 = Os$

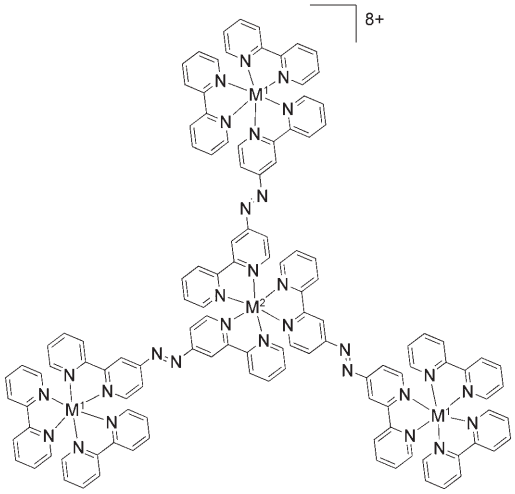

Ru_4: $M^1 = M^2 = Ru$
Ru_3Os: $M^1 = Ru$, $M^2 = Os$

The redox-responsive light switches have been extended to switches for energy transfer; for the cases of Ru/Os heteronuclear complexes containing one of the azo ligands, the excited state of the as-prepared complexes deactivates without luminescence, while the reduced counterparts exhibit intramolecular excited energy transfer from the Ru unit to the Os unit,[1c,9] from which luminescence is emitted (see the top reaction in Figure 1).[3d,f,g] Such energy transfer plays a pivotal role at the initial stage of photosynthesis.[10] Thus, extensive efforts have so far been devoted to develop antenna systems that can harness solar energy.[11] However, no switch function has been introduced in such antenna systems.[12]

We report herein a first switchable antenna, composed of a heterotetranuclear complex, $[\{(bpy)_2Ru(azobpy)\}_3Os]^{8+}$ (**Ru_3Os**), which contains an Os unit in the center as an energy accepting site surrounded by three peripheral Ru units as light absorbing sites. The energy collection is switched on and off depending on the redox state of the ligands bridging the central and peripheral metal complexes.

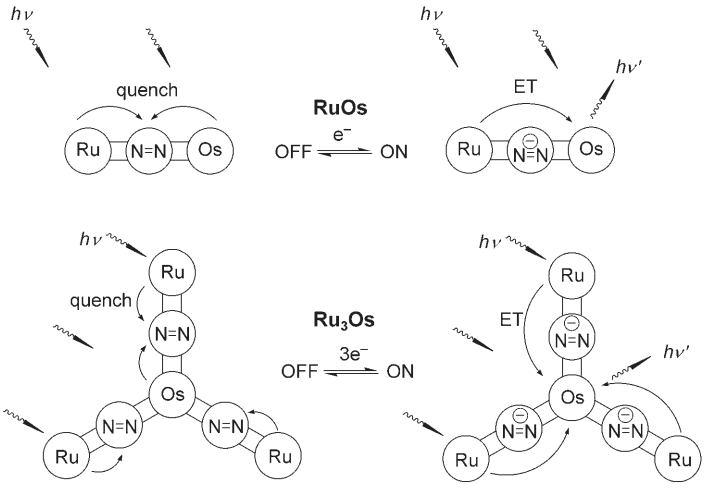

Figure 1. Conceptual schemes for a switch for intramolecular energy transfer (**RuOs**) and a switchable antenna (**Ru_3Os**). ET stands for energy transfer.

Increasing the number of light absorbing sites leads to an increased absorptivity, resulting in an antenna effect (see the bottom reaction in Figure 1). We examined the detailed photodynamics of the redox-responsive switchable antenna function of **Ru_3Os** by using femtosecond laser flash photolysis.

Results and Discussion

Structural characterization: All ^1H NMR spectroscopy resonances were assigned with the help of the ^1H–^1H COSY spectrum in Figure 2 and the comparison with the spectrum

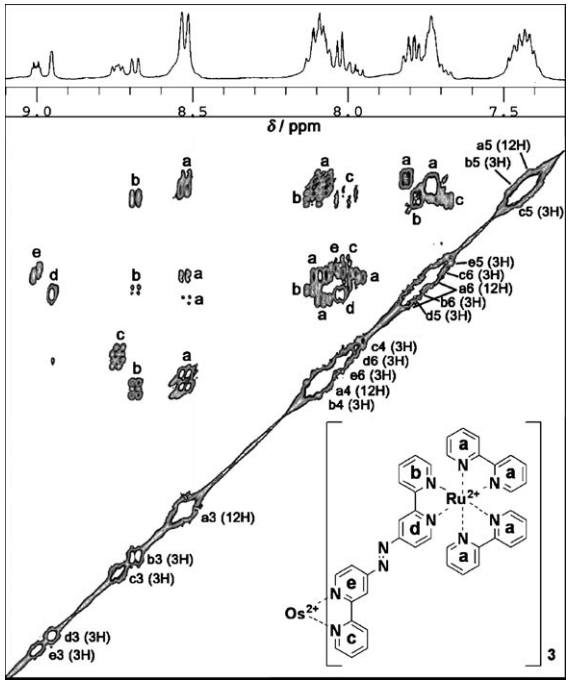

Figure 2. ^1H–^1H NMR COSY spectrum for **Ru_3Os** in CD_3CN.

of **Ru_4**.[3e] All protons within each pyridyl ring are spin–spin coupled. Thus, each of the off-diagonal peaks in the COSY spectrum can be attributed to nearly equivalent pyridyl rings, as indicated by letters a–e in Figure 2. The chemical shifts for protons in rings a, b, and d of the peripheral Ru complexes are nearly identical to those of corresponding protons in **Ru_4**,[3e] as expected. The differences in chemical shifts for **Ru_3Os** and **Ru_4** are observed for the protons in rings e and c, and reflect the influence of the different central metal ion. These consistent agreements between the observed chemical shifts and the assumed structure provide a strong support for the structure of **Ru_3Os**.

The obtained complex must be a mixture of many structural isomers, since it contains four stereo (*fac* and *mer*) and optical (D and L) isomeric centers. Differences in chemical shifts among these isomers seem to be small, except for the protons at the 6-position of the pyridine rings, which are the most proximal to another ligand within the complex and, therefore, their chemical shifts are most sensitive to the differences among isomers.[3e,13] This is most apparent for the chemical shifts of the a6-protons, which scatter around $\delta =$ 7.7–7.8 ppm. It is generally accepted that electrochemical and spectroscopic differences among these isomers is minimum.[14]

The chemical formula of **Ru_3Os**, was evident from electrospray mass spectrometry (ESMS) (Figure S1 in the Supporting Information). The spectrum shows two major clusters of peaks that indicate the distribution of the isotopes of Ru and Os. The peaks centered at $m/z = 1658$ and 1057 correspond to the species $[M-2(PF_6)]^{2+}$ and $[M-3(PF_6)]^{3+}$, respectively, and a weaker cluster centered at 3461, corresponds to $[M-PF_6]^{+}$. The 1658 cluster is magnified in Figure S1, together with the simulated isotope distribution of **Ru_3Os**. The excellent agreement confirms the composition of **Ru_3Os** and excludes the formation of the hydrazo form,[15] which would give clusters shifted to the higher mass side by six mass units. Finally, CHN analysis agreed within 0.4% with the calculated values as an octahydrate. The octahydrate **Ru_4** complex has previously been obtained.[3e]

Redox properties: The cyclic voltammogram for **Ru_3Os** shows oxidation waves at 0.94 and 0.63 V vs Fc^+/Fc in CH_3CN as shown in Figure 3a. The former value corresponds to the oxidation of the three peripheral Ru ions (+2/+3), virtually at the same potential as in **Ru_4** (0.96 V), whereas the latter value corresponds to the oxidation of the central Os ion (+2/+3). In the cathodic scan in DMF (Figure 3b), redox couples appear at −0.7 and −1.2 V with shoulder waves around −1.5 V. The wave at −0.7 V likely contains three, one-electron reduction processes for the three azobpy bridging ligands. This assignment is based on comparison with analogous complexes,[3a,d,e] and the spectroelectrochemical results, in which reduction at −0.88 V has the same effect as chemical reduction with three equivalents of a reductant (vide infra).

The peak separation of this wave at −0.7 V is ≈200 mV, which is much larger than the value of ≈60 mV expected for a reversible electrode reaction for multiple noninteracting equivalent redox centers.[16] This can be, in principle, a result of the overlapping redox couples at slightly differing potentials, and/or a slow electrode reaction. The peak separation was invariant under different scan rates in the range of 50–200 mV s^{-1}. This result indicates that the redox reaction is indeed fast, to the extent that the electrode reaction is diffusion limited. It leaves only the possibility that the reduction potentials of respective azobpy ligands are slightly different. The difference may result from different diastereomers (vide supra) and/or an overall electrostatic effect, owing to charge accumulation. The electrostatic interaction is, however, much weaker than that is seen among bpy ligands in parent $[M(bpy)_3]^{2+}$-type complexes. For example, three consecutive reductions occur as well separated waves with ≈200 mV differences between the waves (a ≈400 mV overall difference) in the cases of $[Ru(bpy)_3]^{2+}$ and $[Os(bpy)_3]^{2+}$. The weaker interaction, in the case of **Ru_3Os**, is a result of the increased distance between the additional electrons on azobpy (in comparison with electrons on bpy) from the Os ion.

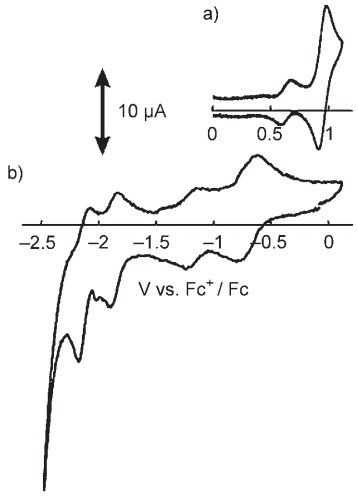

Figure 3. Cyclic voltammogram for **Ru_3Os**. The anodic scan a) was performed in CH_3CN, while the cathodic scan b) was in DMF.

The waves around −1.2 to −1.5 V may correspond to the second, one-electron reduction of the monoanions of azobpy to form dianions.[17] The reduction waves of the peripheral bpy ligands appear at < -1.8 V. This makes it possible to inject electrons into the azobpy ligand selectively, which is important when this complex is used as a redox-responsive switch, as discussed later.

Absorption and luminescence: Ru polypyridine complexes, such as $[Ru(bpy)_3]^{2+}$, exhibit characteristic ^{1}MLCT absorption band (Ru→bpy) around $\lambda = 450$ nm.[18] In this transition, a dπ electron is promoted into the π* orbital of one of the bpy ligands. The Os counterparts, such as $[Os(bpy)_3]^{2+}$, also exhibit the ^{1}MLCT absorption in a similar wavelength range. In addition to this spin-allowed transition, Os polypyridine complexes feature a weaker, but substantial, spin-

forbidden ^{3}MLCT absorption in the $\lambda = 500$–700 nm region, owing to the heavy atom effect.[18] Consistent with the low-lying π^* level of azobpy, the complexes containing azobpy show additional MLCT transition bands ($M^{II} \rightarrow$azobpy) at the lower energy side by $\approx 5000\ cm^{-1}$ of the MLCT bands of the parent complex having only bpy ligands.[3a,d,e]

The electronic absorption spectrum for **Ru_3Os**, which is shown by the solid line in Figure 4, includes all of these transitions. According to the above criteria, the bands are

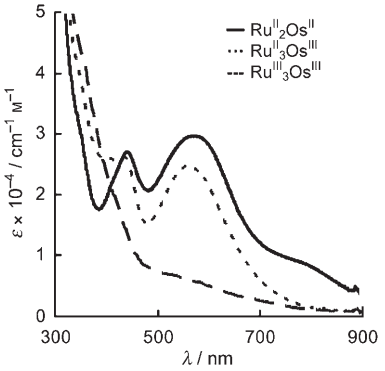

Figure 4. Absorption spectra in CH_3CN for the as-prepared **Ru_3Os** (——), the one-electron oxidized species (0.82 V; ·····), and the four-electron oxidized species (1.22 V; – – –).

assigned as follows. The $\lambda = 440$ nm band ($\varepsilon = 26\,000\ M^{-1}\ cm^{-1}$) is assigned to the ^{1}MLCT (Ru/Os $\rightarrow$ bpy) transitions. The lower energy $\lambda = 580$ nm band ($30\,000\ M^{-1}\ cm^{-1}$) includes the ^{1}MLCT (Ru/Os $\rightarrow$ azobpy) and the spin-forbidden ^{3}MLCT (Os $\rightarrow$ bpy) transitions. Finally, the band even lower in energy around $\lambda \approx 800$ nm ($8000\ M^{-1}\ cm^{-1}$) corresponds to the ^{3}MLCT (Os$\rightarrow$azobpy) transition.

These assignments are supported by spectroelectrochemical experiments, in which 1) Os^{II} is oxidized to Os^{III}, 2) the Ru^{II} centers are oxidized to Ru^{III} centers and 3) the azobpy ligands are reduced to their respective monoanions. Upon selective oxidation of the Os ion by applying 0.82 V, the absorption bands uniformly decrease in the whole visible range above $\lambda = 480$ nm (Figure 4, dotted line). Notably, the absorption almost disappears in the $\lambda = 800$–900 nm range, in which only Os-related transitions are exhibited. Indeed, the shape of the absorption spectrum of this species, $[\{(bpy)_2Ru^{II}(azobpy)\}_3Os^{III}]^{9+}$ is nearly identical to that of **Ru_4** below $\lambda = 900$ nm.[3e] However, a new absorption plateau ($\varepsilon = \approx 800\ M^{-1}\ cm^{-1}$) appears above $\lambda = 900$ nm, as shown by the difference spectrum in Figure S2 in the Supporting Information (dotted line), which may be assigned to the Ru^{II} to Os^{III} intervalence charge transfer band.[12] Upon further oxidation by applying 1.22 V, the whole MLCT absorption in the visible region nearly completely disappears (Figure 4, dashed line), as a result of the oxidation of all metal centers. The plateau above $\lambda = 900$ nm also disappears (Figure S2, dashed line).

This species is nearly non-luminescent ($< 0.3\,\%$ of the luminescence of $Ru(bpy)_3{}^{2+}$) at least up to $\lambda = 900$ nm, which is the limit of our luminescence detector, as is the case for other complexes containing the azobpy ligand.[19]

Transient absorption: When $[Ru(bpy)_3]^{2+}$ is excited in the visible absorption band, the ^{1}MLCT states would be initially created as the Franck–Condon states, in which one of the dπ electrons is promoted to a delocalized or localized π^* orbital of the ligand(s). The ^{1}MLCT states rapidly relax into the lowest excited ^{3}MLCT state. The relaxation completes within 300 fs in CH_3CN, with the processes of intramolecular vibrational relaxation, solvent reorganization, and intersystem crossing all occurring simultaneously.[20] In the case of $[Os(bpy)_3]^{2+}$, the initially created species depends on the excitation wavelength, because direct excitation into either the ^{1}MLCT or ^{3}MLCT is possible, owing to a stronger spin-orbit coupling. Even if ^{1}MLCT is initially created with a short wavelength of light, the intersystem crossing to the ^{3}MLCT occurs rapidly (< 1 ps), which is followed by vibrational relaxation within the triplet manifold in 16 ps.[21] In mixed ligand complexes in the ^{3}MLCT state, the promoted electron is localized on a π^* orbital with the lowest energy. For **Ru_3Os**, the ^{3}MLCT states may be formally represented as $[\{(bpy)_2Ru^{II}(azobpy)\}_2(bpy)_2Ru^{III}(azobpy^{\bullet-})Os^{II}]^{8+}$ and $[\{(bpy)_2Ru^{II}(azobpy)\}_2(bpy)_2Ru^{II}(azobpy^{\bullet-})Os^{III}]^{8+}$, which correspond to Ru-based and Os-based excited states, respectively.

The detailed information about the ^{3}MLCT states was provided by ultrafast time-resolved transient absorption spectroscopy with a femtosecond laser. Figure 5a shows the transient absorption spectra for **Ru_3Os** taken in CH_3CN. The transient spectrum 1 ps after a laser excitation consists of positive absorption in the ranges of $\lambda < 500$ nm and 650–800 nm and a bleaching in the 500–650 nm range. The absorption at $\lambda < 500$ nm may be ascribed to the MLCT band involving $M^{II} \rightarrow azobpy^{\bullet-}$ ($M^{II} = Ru^{II}$, Os^{II}) transitions, because the same absorption band is seen in the three-electron reduced **Ru_3Os** (vide infra). The dip at $\lambda = 440$ nm may be ascribed to the disappearance of the MLCT band of $Ru^{II} \rightarrow$ bpy from the ground state spectrum. The bleaching in the $\lambda = 500$–650 nm region is, owed to the disappearance of the large MLCT bands involving $M^{II} \rightarrow$azobpy transitions in this range. The long wavelength absorption in the region $\lambda = 700$–800 may be ascribed to radical anions, $bpy^{\bullet-}$ and $azobpy^{\bullet-}$. The absorbance at $\lambda = 770$ nm decays with a lifetime (τ) of 0.40 ps (Figure 5b, △), leaving a plateau-like absorption around $\lambda = 660$–720 nm. The difference spectral profile produced by subtracting the 3.0 ps spectrum from the 1.0 ps spectrum closely resembles the reported transient spectrum of $bpy^{\bullet-}$.[22] Thus, the transition with the 0.4 ps lifetime is attributable to the interligand electron transfer from $bpy^{\bullet-}$ to azobpy to produce $azobpy^{\bullet-}$.[23] A rise in absorbance at $\lambda = 460$ nm (Figure 5b, ●) accompanies the transition with the same time constant of 0.4 ps. This rise corroborates the formation of $azobpy^{\bullet-}$. Thus, the formation of the MLCT states of $Ru(bpy)_2$-based and $Os(bpy)_2$-based excited states upon

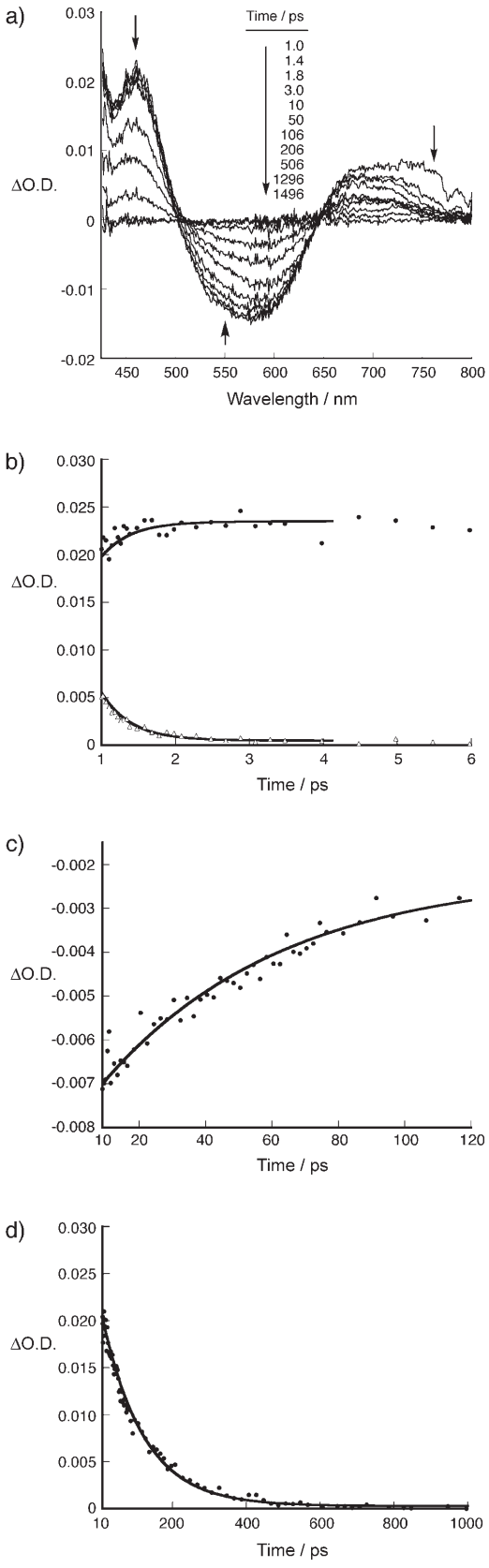

Figure 5. Time evolution of transient absorption for **Ru_3Os** in CH_3CN. a) Spectral changes upon excitation at $\lambda = 410$ nm. Time profiles of absorbance at selected wavelengths with different timescales at b) $\lambda = 460$ (●) and 770 (△), c) 550, and d) 460 nm.

photoexcitation is followed by rapid electron transfer from the $bpy^{\bullet-}$ radical anion to azobpy, giving rise to $[\{(bpy)_2Ru^{II}(azobpy)\}_2(bpy)_2Ru^{III}(azobpy^{\bullet-})Os^{II}]^{8+}$ and $[\{(bpy)_2Ru^{II}(azobpy)\}_2(bpy)_2Ru^{II}(azobpy^{\bullet-})Os^{III}]^{8+}$.

Notably, the maximum wavelength of the bleaching is shifted from $\lambda = 575$ nm to 590 nm in the recovery process, because the rate of increase in absorption in the bleach region is wavelength dependent. Thus, the increase at $\lambda = 550$ nm (Figure 5c) is much faster than that at 590 nm, which is indicative of the transformation of the Ru-based MLCT excited state to the Os-based MLCT excited state, as these wavelengths correspond to the maxima of the $Ru^{II} \rightarrow$azobpy and $Os^{II} \rightarrow$azobpy bands, respectively, in the ground state absorption spectra.[3d] This is an energy transfer process from the Ru-based excited state to the Os-based excited state. This process may also be regarded as a metal-to-metal electron transfer ($Ru^{III} + Os^{II} \rightarrow Ru^{II} + Os^{III}$). The lifetime of the energy-transfer process can be estimated to be 54 ps from the recovery of the bleaching at $\lambda = 550$ nm (Figure 5c). Although the energy transfer does occur, it is between the low-energy nonemitting states in which the excited electron is located in azobpy. Finally, in the slowest process, the whole transient species decays back to the ground state with a lifetime of 113 ps, which is determined from the decay time profile of absorbance at $\lambda = 460$ nm (Figure 5d). The lifetime is considerably shortened in comparison with the lifetime of the parent complex, $[Os(bpy)_3]^{2+}$ (20 ns)[24] owing to the presence of the azobpy ligands. Figure 6a shows the energy diagram for the relevant MLCT states.

Redox-responsive switching: The absorbance of the lower-energy bands of **Ru_3Os** is diminished after the electrolysis at -0.88 V for one-electron reduction (Figure 7). This spectrum strongly suggests that the transitions to the lowest π^* orbitals of the azobpy ligands are now prohibited. Thus, at this electrode potential, it is likely that all three azobpy ligands in the complex are one-electron reduced, **Ru_3Os^R**. This change can be reversed by re-oxidizing **Ru_3Os^R** back to **Ru_3Os**, thus restoring the original absorption spectrum. The reduction of **Ru_3Os** can also be effected by chemical reductants. If a **Ru_3Os** solution in DMF[26] is titrated with cobaltocene then a spectral change identical to that by the electrochemical reduction is observed. The spectral changes were completed after three equivalents of cobaltocene were added to the solution. This indicates that the one-electron reduction for each azobpy is responsible for the spectral change (Figure S3 in the Supporting Information). Further addition of cobaltocene did not bring about any further spectral changes. The chemical reduction by means of tetramethylsemiquinone radical anion as a reductant also gave a similar spectral change. The change upon reduction is rationalized by assuming that the MLCT transitions ($M^{II} \rightarrow$ azobpy) are now prohibited, since electrons occupy the lowest π^* orbitals of the azobpy ligands.

To confirm the site of the one-electron reduction of **Ru_3Os**, the singly-occupied molecular orbital (SOMO) of one-electron reduced **Ru_3Os** ($[\{(bpy)_2Ru(azobpy)\}_3Os]^{7+}$)

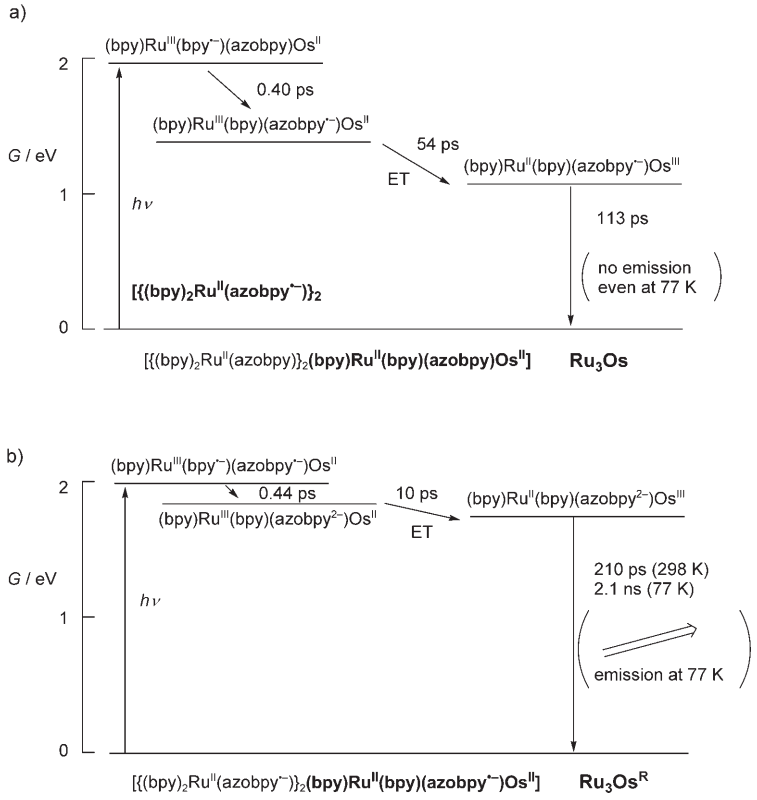

Figure 6. Energy diagrams of the redox-responsive switchable antenna based on MLCT states of a) **Ru_3Os** and b) **Ru_3Os^R**.[25] A shorthand notation is used for each excited state, in which only a part of the complex (bold-faced in the ground state description), is shown. ET stands for energy transfer. Direct excitation of the Os-based unit is omitted for clarity.

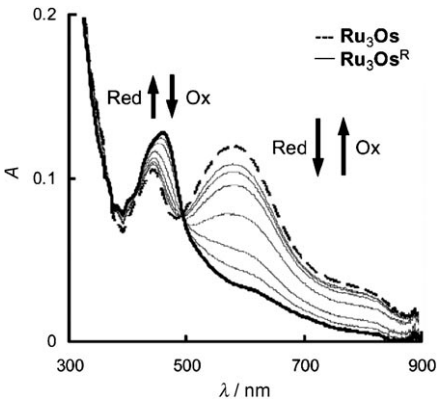

Figure 7. Changes in the absorption spectrum for **Ru_3Os** (40 μM) in DMF upon reduction at −0.88 V and re-oxidation in a 1 mm cuvette.

has been calculated by density functional theory (Figure 8). The structure was optimized by using the Gaussian03 program package (see the Experimental Section). The SOMO is mainly localized on the bridging three azobpy's, wherein the density is largely located on the N=N moiety. Therefore, these bridging ligands are the site where the first reduction takes place, at the least negative potential.

The three-electron reduced species, **Ru_3Os^R** is nearly non-luminescent, similar to the as-prepared **Ru_3Os** at room temperature. This is in sharp contrast to **Ru_4**[3e] and other related complexes for which the same electrolysis produces an appreciable luminescence. Considering the fact that the chemical environment of the peripheral three Ru units is the same in **Ru_4^R** and **Ru_3Os^R**, an efficient quenching mechanism unique to the excited Ru units in **Ru_3Os^R** must be in operation. The most likely quenching mechanism is energy transfer to the central Os unit. However, we did not observe the expected luminescence from the excited Os unit as observed for the dinuclear **$RuOs^R$**,[3d] which would be produced by the energy transfer in addition to the direct excitation. This may be explained by a low quantum yield of $[Os(bpy)_3]^{2+}$ unit ($\varphi = \approx 0.005$).[18b] This value could be lowered further by the azo substitution on all of the three bipyridine ligands[27] and by the reductive electron transfer from the reduced azobpy ligands to the emptied Os d-orbital in the MLCT excited state. Then, the luminescence was measured at 77 K by transferring the electrolyzed solution to a quartz tube cooled in a liquid nitrogen jacket. The cooled luminescence spectra taken for **Ru_3Os** and **Ru_3Os^R** are compared in Figure 9a. The $\lambda = 650$ nm peak for the as-prepared **Ru_3Os** is a weak residual Ru-based luminescence, which appeared probably because electron transfer from $bpy^{\cdot-}$ radical anion to azobpy may be slowed down at 77 K. Upon reduction, the Ru-based luminescence ($\lambda = 650$ nm) showed no increase in intensity, whereas for the Os-based luminescence a peak at $\lambda =$ 743 nm appears. This observation is indicative of an energy transfer process from the Ru-based to the Os-based excited states. Energy transfer in **Ru_3Os^R** is corroborated by its excitation spectrum at 77 K monitored at $\lambda = 743$ nm where the Os-based luminescence dominates, as given in Figure 9b (solid line). The excitation spectra for reduced dinuclear complexes, **$RuOs^R$** and **Os_2^R**,[3d] measured at room temperature are also shown. Comparison of the spectra reveals that the luminescence from the Os unit with excitation at the shorter wavelength region ($\lambda = 450$–550 nm), where the Ru-based unit absorbs more, is enhanced for **$RuOs^R$** as compared to **Os_2^R**. This demonstrates the sensitization of the luminescence from the Os unit by the Ru unit in the heterodi-

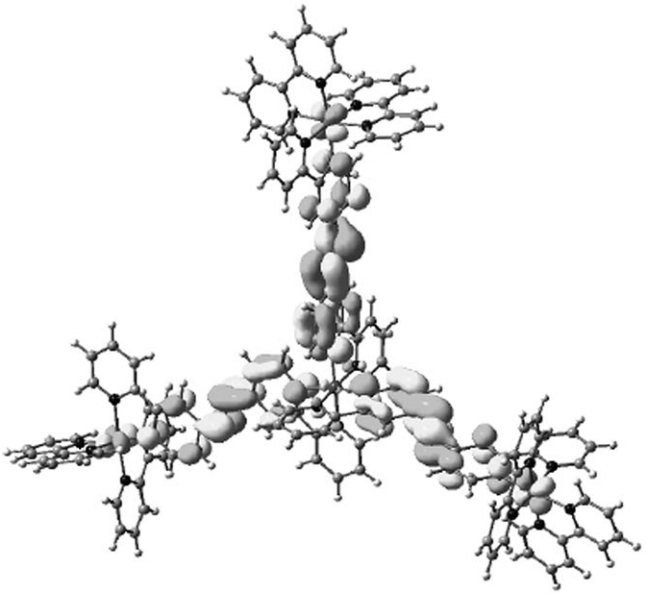

Figure 8. The SOMO of $[\{(bpy)_2Ru(azobpy)\}_3Os]^{7+}$ calculated with Gaussian 03.

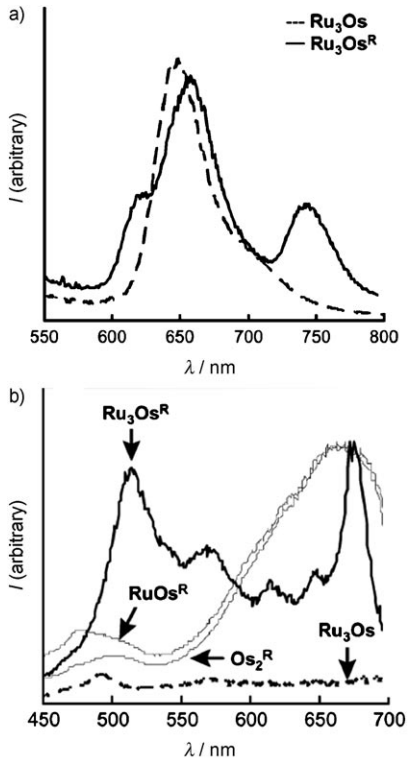

Figure 9. Luminescence response of **Ru_3Os** (10 μM) to redox input in DMF containing 0.1 M Bu_4NPF_6 at 77 K. a) Luminescence spectra for **Ru_3Os** (– – –) and **Ru_3Os^R** (——). $\lambda_{ex}=495$ nm (isosbestic point). b) Excitation spectra for **Ru_3Os** (– – –) and **Ru_3Os^R** (——) monitored at $\lambda=$ 743 nm. The excitation spectra for reduced dinuclear complexes, **$RuOs^R$** and **Os_2^R**, at room temperature are also shown for comparison. The intensities are normalized at $\lambda=675$ nm.

nuclear complex. The enhancement is even more pronounced for the tetranuclear complex, **Ru_3Os^R**, and shows the antenna effect for the energy transfer process.

Time-resolved luminescence measurements for **Ru_3Os^R** at 77 K showed that the decay at around $\lambda=650$ nm, where the Ru luminescence dominates, is a single exponential with a lifetime of $\tau=2.1$ ns. This lifetime is much shorter than that of **Ru_4^R** (186 ns at room temperature),[3e] indicating an energy transfer process with an efficiency near unity.[28] This is also supported by the steady-state luminescence experiments described above. First, the reduction-induced enhancement in the Ru-based luminescence in **Ru_3Os** is negligible in contrast to that in **Ru_4** at room temperature.[3e] Second, only the Os-based luminescence is enhanced at 77 K (Figure 9a). A model experiment using **Ru_4** showed that the luminescence of **Ru_4** is enhanced ≈30-fold upon reduction under the same low-temperature conditions ($\lambda_{max}=$ 630 nm).

The mechanistic insight into the apparent energy-transfer process in **Ru_3Os^R** is also provided by ultrafast time-resolved transient absorption spectroscopy with a femtosecond laser. Figure 10a,c shows the transient absorption spectra for **Ru_3Os^R** taken in DMF, which are quite different from those observed for **Ru_3Os** in Figure 5a. The transient spectra consist of a bleaching at $\lambda=460$ nm and broad absorption bands at $\lambda=580$ nm and 770 nm. The time profiles of the absorbance at 410, 580 and 770 nm (Figure 10b,d,e) exhibit a three step processes. The first process (1.2–4.0 ps), in which the broad absorption at $\lambda>550$ nm increases, may correspond to electron transfer from the $bpy^{\bullet-}$ radical anion of the MLCT ($Ru^{II}\rightarrow bpy$) to the $azobpy^{\bullet-}$ to produce $azobpy^{2-}$ (Figure 6b) exhibiting the first-order rise with $\tau=0.44$ ps (Figure 10b). As the unpaired electron of $azobpy^{\bullet-}$ in **Ru_3Os^R** is largely localized on the N=N moiety (vide supra), a second electron may be largely delocalized on the two bpy units of azobpy. Such extended delocalization over two bpy units through the N=N moiety is responsible for the broad absorption bands at $\lambda=580$ and 770 nm. Similar features are reported for radical anions of other conjugated structures including bpy units.[29–31] This assignment is also consistent with an energetic standpoint, as the one-electron reduction potential of $azobpy^{\bullet-}$ is less negative than that for the one-electron reduction of bpy. The second process (4.5–50 ps) may correspond to a metal-to-metal electron transfer ($Ru^{III}+Os^{II}\rightarrow Ru^{II}+Os^{III}$) to afford the Os-based excited state as the final MLCT state (Figure 6b) as observed for **Ru_3Os** (Figure 6a), which exhibits the first-order rise at $\lambda=460$ nm (owing to the reappearance of the MLCT bands, $Ru^{II}\rightarrow bpy$ and $Ru^{II}\rightarrow azobpy^{\bullet-}$) and the decay at $\lambda=580$ nm (owing to the disappearance of the MLCT band, $Os^{II}\rightarrow azobpy^{\bullet-}$) (Figure 10d) with the same lifetime of $\tau=10$ ps. This electron transfer process for **Ru_3Os^R** is equivalent to the energy transfer from the Ru unit to the Os unit. The last step is the decay of the MLCT state to the ground state exhibiting the first-order rise at $\lambda=460$ nm and the decay at 770 nm (Figure 10e) with the same lifetime of $\tau=210$ ps. The lifetime of the final MLCT state of **Ru_3Os^R** (210 ps) is longer than that of **Ru_3Os** (113 ps).

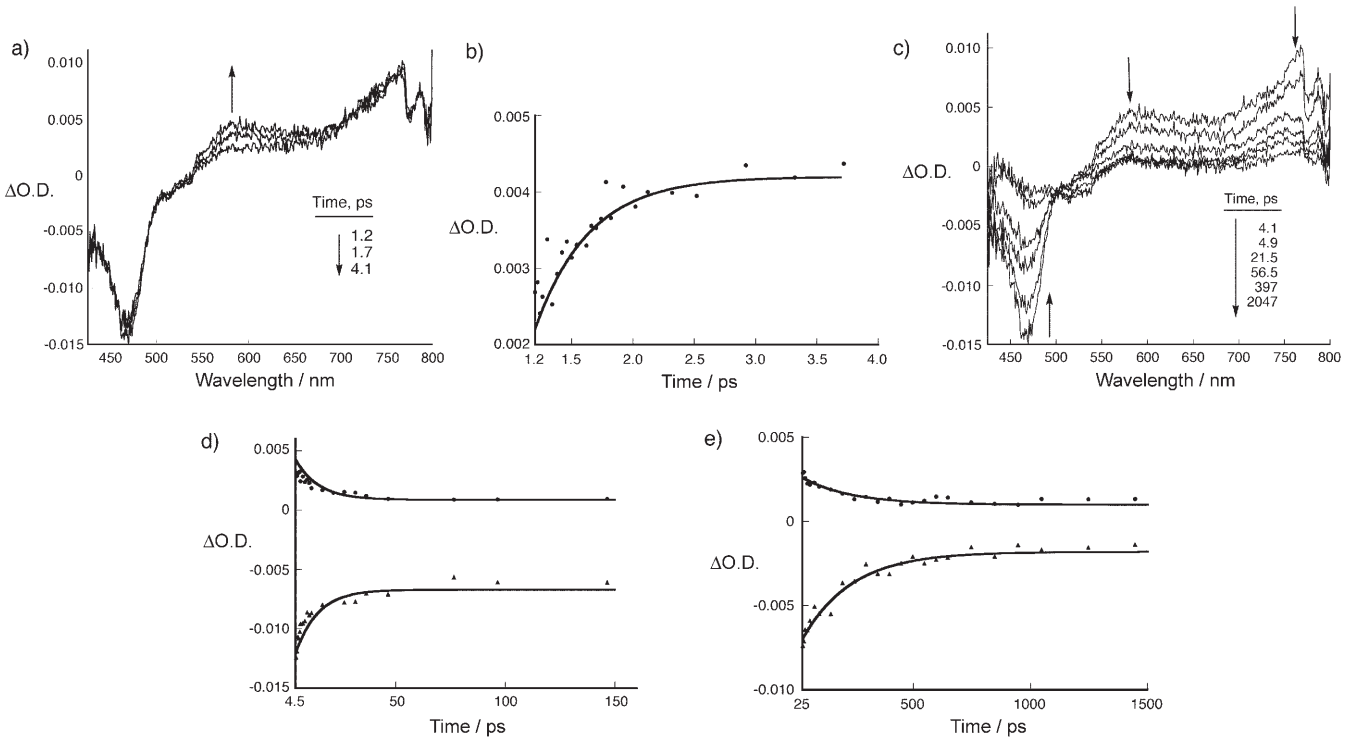

Figure 10. Time evolution of transient absorption for $\mathbf{Ru_3Os^R}$ in DMF. a) Spectral changes upon excitation at $\lambda = 410$ nm for 1.2–4.0 ps and b) the time profile at 580 nm. c) Spectral changes after 4.1 ps and time profiles at d) 580 (●) and 460 nm (▲). e) Time profiles at $\lambda = 460$ (▲) and 770 nm (●) at prolonged timescale (25–1500 ps).

Conclusion

The star-shaped **Ru_3Os** works as a switchable antenna. In the as-prepared off-state, the photoexcited states are largely quenched, owing to the presence of low-lying π* levels of the azobpy ligands. Although an energy-transfer process does occur from an Ru-based excited state to an Os-based excited state, this process is between low-lying nonemitting states, in which the excited electron is in one of the azobpy ligands in the form of azobpy$^{\bullet-}$. In the on-state, on the other hand, a highly efficient energy-transfer process from the periphery to the center is indicated, based on the quenching of the Ru emission at room temperature. This is more clearly evidenced by a sensitized Os-based luminescence at 77 K. The apparent energy-transfer results from two steps: intramolecular electron transfer from bpy$^{\bullet-}$ to azobpy$^{\bullet-}$ to form azobpy^{2-} followed by a metal-to-metal electron transfer ($Ru^{III}+Os^{II} \rightarrow Ru^{II}+Os^{III}$) as revealed by ultrafast time-resolved transient absorption measurements.

Experimental Section

General: Chemicals were purchased from commercial sources and used without further purification, unless otherwise noted. The solvents CH_3CN and CH_2Cl_2 were distilled over CaH_2 before use.

Apparatus: ^{1}H NMR spectra were recorded on a JEOL GX400 spectrometer. Electrospray mass spectrometry (ESMS) analysis was conducted by using a Agilent G1969A system with a time-of-flight mass spectrometer. Elemental analyses were carried out at the Analysis Center of College of Science and Technology, Nihon University. UV-visible data were obtained by using a Shimadzu UV-2400PC or Multispec-1500 spectrometer. Luminescence spectra were recorded on a Shimadzu RF-5300PC fluorimeter. Near infrared spectra were recorded with a Shimadzu UV-3100PC.

Electrochemical measurements: Electrochemical measurements were carried out by using a Hokuto Denko HZ-3000 voltammetric analyzer. The working and counter electrodes were a Pt disk and a Pt wire, respectively. The reference electrode was either Ag/Ag^+ (0.01 M $AgNO_3$ and 0.1 M NH_4PF_6 in CH_3CN) or an Ag wire pseudoreference. Potentials are reported with respect to the internal ferricenium/ferrocene couple (Fc^+/Fc) added after each measurement. The supporting electrolyte solution was 0.1 M Bu_4NPF_6 in CH_3CN or DMF (Wako, Infinity Pure). All measurements were done under a Ar blanket.

Spectroelectrochemical and time-resolved luminescence measurements: Absorption and luminescence spectroelectrochemical measurements were performed in CH_3CN (oxidation) or DMF with a drop of aqueous HNO_3 (reduction) containing 0.1 M Bu_4NPF_6 in an optical cuvette with a 1 cm or 1 mm optical path length. The cell was equipped with a Pt mesh, an Ag/Ag^+, and a Pt coil separated with an absorbent cotton, as the working, reference, and counter electrodes, respectively. The cell was purged and then blanketed with Ar. The sample solution in the 1 cm cuvette was being stirred during electrolysis. For low temperature measurements, the electrolyzed solution was transferred into a quartz tube placed in a liquid N_2 jacket. Time-resolved luminescence decay for reduced species was measured with excitation by pulses through a coumarin chromophore ($\lambda = 447$ nm) from a nitrogen laser ($\lambda = 337$ nm) at 77 K. The emission was then dispersed by means of a Hamamatsu Photonics C-2830 disperser and monitored by using a Hamamatsu Photonics M-2548 streak camera.

Laser flash photolysis: Ultrafast transient absorption spectroscopy experiments were conducted by using an ultrafast source: Integra-C (Quan-

tronix Corp.), an optical parametric amplifier: TOPAS (Light Conversion Ltd.) and a commercially available optical detection system: Helios provided by Ultrafast Systems LLC. The source for the pump and probe pulses were derived from the fundamental output of Integra-C (780 nm, 2 mJ/pulse and fwhm = 130 fs) at a repetition rate of 1 kHz. 75% of the fundamental output of the laser was introduced into TOPAS, which has optical frequency mixers resulting in tunable range from $\lambda = 285$ nm to 1660 nm, whereas the rest of the output was used for white light generation. Prior to generating the probe continuum, a variable neutral density filter was inserted in the path in order to generate stable continuum, then the laser pulse was fed to a delay line that provides an experimental time window of 3.2 ns with a maximum step resolution of 7 fs. In our experiments, a wavelength between $\lambda = 350$ nm and 450 nm of TOPAS output, which is fourth harmonic of signal or idler pulses, was chosen as the pump beam. As this TOPAS output consists of not only desirable wavelength but also unnecessary wavelengths, the latter wavelengths were deviated by using a wedge prism with wedge angle of 18°. The desirable beam was irradiated at the sample cell with a spot size of 1 mm diameter where it was merged with the white probe pulse in a close angle (< 10°). The probe beam after passing through the 2 mm sample cell was focused on a fiber optic cable, which was connected to a CCD spectrograph for recording the time-resolved spectra ($\lambda = 410$–800 nm). Typically, 2500 excitation pulses were averaged for 5 seconds to obtain the transient spectrum at a set delay time. Kinetic traces at appropriate wavelengths were assembled from the time-resolved spectral data. All measurements were conducted at room temperature, 295 K.

Chemical reduction: Chemical reduction by cobaltocence[32] (Wako) was effected by adding aliquots of a deaerated cobaltocene solution in DMF or CH_3CN to a deaerated solution of Ru_3Os in DMF containing a small amount of aqueous HNO_3. The absorption spectra were recorded after each addition. The exact concentration of added cobaltocene was determined by reducing a methyl viologen (MV^{2+}) ($MV^{\bullet+}$: $\varepsilon = 1.24 \times 10^4\,M^{-1}\,cm^{-1}$ at $\lambda = 603$ nm) solution.[33] Chemical reduction was also carried out by using tetramethylsemiquinone radical anion as a reductant, which was obtained by a proportionation reaction of tetramethyl-*p*-benzoquinone (Wako) with tetramethylhydroquinone dianion that had been formed by the reaction of tetramethylhydroquinone (TCI) with tetramethyl-ammonium hydroxide (Nacalai Tesque).[34]

Preparation of azobpy: The preparation of azobpy has been improved significantly from a previously reported method,[13] as described herein. A suspension of 4-nitro(2,2′-bipyridine)[35] (323 mg, 1.61 mmol) in 2-propanol (40 mL) was refluxed. After the suspension became clear, an aqueous solution of NaOH (1.1 g/2 mL) was added, and then Zn powder (2.7 g) was added portionwise over a period of 5 min. After another 3 h reflux, the reaction mixture was cooled with an ice bath. The resultant solid was collected on filter paper, washed with hot H_2O and EtOH, and then extracted with hot $CHCl_3$. The removal of $CHCl_3$ afforded an orange solid (155 mg, 0.46 mmol, 57%), which was suitable for use in the preparation of $[(bpy)_2Ru(azobpy)](PF_6)_2$[3a] without further purification. The characterization data for azobpy are given in ref. [3na].

Preparation of Ru_3Os: K_2OsCl_6 (30 mg, 0.06 mmol) was dissolved in ethyleneglycol (30 mL) at 100 °C under Ar. Then, $[(bpy)_2Ru(azobpy)](PF_6)_2$ (200 mg, 0.2 mmol) was added to this solution, which was then heated at 160 °C for 4 h. The solution was cooled to room temperature, to which H_2O (20 mL) and excess NH_4PF_6 were added. The precipitate was collected, washed with a small amount of H_2O and ether. The solid was chromatographed on SiO_2 eluted with CH_3CN/0.4 M aqueous KNO_3 (3/1). A blue-green band was collected and the CH_3CN was gently evaporated to leave an aqueous solution, to which excess NH_4PF_6 was added. The precipitate was collected, washed with a small amount of H_2O and ether, and dried under vacuum to afford dark green powder. This solid was dissolved in CH_3CN, to which trifluoroacetic acid (20 mL) was added. The solvent was removed under reduced pressure and the resulting dark blue powder was dried under vacuum. This was dissolved in a mixture of H_2O and CH_3CN containing NH_4PF_6. Mild evaporation of CH_3CN gave a precipitate, which was washed with a small amount of H_2O and ether, and dried under vacuum to afford a dark blue solid (14 mg, 6%). ^1H NMR (400 MHz, CD_3CN, TMS): $\delta = 9.00$ (m, 3H), 8.95 (m, 3H), 8.74 (m, 3H), 8.68 (d, ^3J (H,H) = 8 Hz, 3H), 8.52 (d, ^3J (H,H) = 8 Hz, 12H), 7.9–8.2 (m, 24H), 7.6–7.8 (m, 24H), 7.3–7.5 ppm (m, 18H); ESMS (CH_3CN): cluster peaks with maxima at *m/z*: 3461 $[(M-PF_6)^+]$, 1658 $[(M-2(PF_6))^{2+}]$, 1057 $[(M-3(PF_6))^{3+}]$; elemental analysis calcd (%) for $C_{120}H_{90}F_{48}N_{30}OsP_8Ru_3 \cdot 8H_2O$: C 38.44, H 2.85, N 11.21; found: C 38.45, H 2.88, N 10.84.

Theoretical calculations: Density functional calculations were performed with Gaussian03 (Revision C.02, Gaussian,) by using the spin-restricted BLYP functional for the open shell molecule[36] on an 8-processor QuantumCubeTM developed by Parallel Quantum Solutions (PQS). The basis set was the double-ζ LanL2DZ, which applies effective core potentials[37] to atoms in the third row and below.

Acknowledgements

This work was partly supported by the High-Tech Research Center Project for Private Universities, MEXT, Japan.

[1] For reviews, see: a) L. Fabbrizzi, A. Poggi, *Chem. Soc. Rev.* **1995**, *24*, 197–202; b) L. De Cola, P. Belser, *Coord. Chem. Rev.* **1998**, *177*, 301–346; c) F. Barigelletti, L. Flamigni, *Chem. Soc. Rev.* **2000**, *29*, 1–12; d) V. Balzani, A. Credi, M. Venturi, *Molecular Devices and Machines - A Journey into the Nano World*, Wiley-VCH, Weinheim, **2003**, Chapter 4, pp. 64–95; e) B. L. Ferringa, *Molecular Switches*, Wiley-VCH, Weinheim, **2001**; f) H. Hofmeier, U. S. Schubert, *Chem. Soc. Rev.* **2004**, *33*, 373–399; g) A. C. Benniston, *Chem. Soc. Rev.* **2004**, *33*, 573–578; h) F. M. Raymo, M. Tomasulo, *Chem. Soc. Rev.* **2005**, *34*, 327–336; i) J. Otsuki, T. Akasaka, K. Araki, *Coord. Chem. Rev.* **2008**, *252*, 32–56.

[2] For recent examples, see: a) V. Amendola, L. Fabbrizzi, P. Pallavicini, E. Sartirana, A. Taglietti, *Inorg. Chem.* **2003**, *42*, 1632–1636; b) J. F. Berry, F. A. Cotton, P. Lei, T. Lu, C. A. Murillo, *Inorg. Chem.* **2003**, *42*, 3534–3539; c) A. C. Benniston, G. M. Chapman, A. Harriman, S. A. Rostron, *Inorg. Chem.* **2005**, *44*, 4029–4036; d) X. Xiao, W. Xu, D. Zhang, H. Xu, H. Lu, D. Zhu, *J. Mater. Chem.* **2005**, *15*, 2557–2561; e) R. Martínez, I. Ratera, A. Tárraga, P. Molina, J. Veciana, *Chem. Commun.* **2006**, 3809–3811; f) I.-W. P. Chen, M.-D. Fu, W.-H. Tseng, J.-Y. Yu, S.-H. Wu, C.-J. Ku, C. Chen, S.-M. Peng, *Angew. Chem.* **2006**, *118*, 5946–5950; *Angew. Chem. Int. Ed.* **2006**, *45*, 5814–5818.

[3] a) J. Otsuki, K. Sato, M. Tsujino, N. Okuda, K. Araki, M. Seno, *Chem. Lett.* **1996**, 847–848; b) J. Otsuki, K. Harada, K. Araki, *Chem. Lett.* **1999**, 269–270; c) J. Otsuki, A. Yasuda, T. Takido, *Chem. Commun.* **2003**, 608–609; d) J. Otsuki, M. Tsujino, T. Iizaki, K. Araki, M. Araki, K. Takatera, T. Watanabe, *J. Am. Chem. Soc.* **1997**, *119*, 7895–7896; e) J. Otsuki, D.-M. Li, K. Sato, A. Nakagome, T. Takido, I. Yoshikawa, T. Akasaka, K. Araki, *Bull. Chem. Soc. Jpn.* **2003**, *76*, 1185–1189; f) T. Akasaka, J. Otsuki, K. Araki, *Chem. Eur. J.* **2002**, *8*, 130–136; g) T. Akasaka, T. Mutai, J. Otsuki, K. Araki, *Dalton Trans.* **2003**, 1537–1544.

[4] a) K. Matsuda, M. Irie, *J. Am. Chem. Soc.* **2001**, *123*, 9896–9897; b) T. Kawai, T. Iseda, M. Irie, *Chem. Commun.* **2004**, 72–73; c) T. Kawai, T. Sasaki, M. Irie, *Chem. Commun.* **2001**, 711–712.

[5] a) Y. Terazono, G. Kodis, J. Andréasson, G. Jeong, A. Brune, T. Hartmann, H. Dürr, A. L. Moore, T. A. Moore, D. Gust, *J. Phys. Chem. B* **2004**, *108*, 1812–1814; b) S. D. Straight, J. Andréasson, G. Kodis, A. L. Moore, T. A. Moore, D. Gust, *J. Am. Chem. Soc.* **2005**, *127*, 2717–2724; c) P. A. Liddell, G. Kodis, J. Andréasson, L. de la Garza, S. Bandyopadhyay, R. H. Mitchell, T. A. Moore, A. L. Moore, D. Gust, *J. Am. Chem. Soc.* **2004**, *126*, 4803–4811; d) J. Andréasson, G. Kodis, Y. Terazono, P. A. Liddell, S. Bandyopadhyay, R. H. Mitchell, T. A. Moore, A. L. Moore, D. Gust, *J. Am. Chem. Soc.* **2004**, *126*, 15926–15927; e) S. D. Straight, J. Andréasson, G. Kodis, S. Bandyopadhyay, R. H. Mitchell, T. A. Moore, A. L. Moore, D. Gust, *J. Am. Chem. Soc.* **2005**, *127*, 9403–9409.

[6] a) J. Otsuki, A. Suka, K. Yamazaki, H. Abe, Y. Araki, O. Ito, *Chem. Commun.* **2004**, 1290–1291; b) J. Otsuki, K. Narutaki, J. M. Bakke, *Chem. Lett.* **2004**, *33*, 356–357; c) J. Otsuki, K. Narutaki, *Bull. Chem. Soc. Jpn.* **2004**, *77*, 1537–1544.

[7] a) R. H. Michell, T. R. Ward, Y. Wang, P. W. Dibble, *J. Am. Chem. Soc.* **1999**, *121*, 2601–2602; b) A. Amini, K. Bates, A. C. Benniston, D. J. Lawrie, E. Soubeyrand-Lenoir, *Tetrahedron Lett.* **2003**, *44*, 8245–8247; c) A. J. Myles, B. Gorodetsky, N. R. Branda, *Adv. Mater.* **2004**, *16*, 922–925; d) A. Hartschuh, I. B. Ramsteiner, H. Port, J. M. Endtner, F. Effenberger, *J. Lumin.* **2004**, *108*, 1–10; e) E. M. Pérez, D. T. F. Dryden, D. A. Leigh, G. Teobaldi, F. Zerbetto, *J. Am. Chem. Soc.* **2004**, *126*, 12210–12211; f) P. Belser, L. De Cola, F. Hartl, V. Adamo, B. Bozic, Y. Chriqui, V. M. Iyer, R. T. F. Jukes, J. Kühni, M. Querol, S. Roma, N. Salluce, *Adv. Funct. Mater.* **2006**, *16*, 195–208; g) R. Sakamoto, M. Murata, H. Nishihara, *Angew. Chem.* **2006**, *118*, 4911–4913; *Angew. Chem. Int. Ed.* **2006**, *45*, 4793–4795.

[8] For reviews, see: a) A. P. de Silva, H. Q. N. Gunaratne, T. Gunnlaugsson, A. J. M. Huxley, C. P. McCoy, J. T. Rademacher, T. E. Rice, *Chem. Rev.* **1997**, *97*, 1515–1566; b) A. P. de Silva, N. D. McClenaghan, *Chem. Eur. J.* **2004**, *10*, 574–586.

[9] V. Balzani, A. Juris, M. Venturi, S. Campagna, S. Serroni, *Chem. Rev.* **1996**, *96*, 759–833.

[10] For natural light harvesting antennas, see: T. Pullerits, V. Sundström, *Acc. Chem. Res.* **1996**, *29*, 381–389.

[11] a) V. Balzani, S. Campagna, G. Denti, A. Juris, S. Serroni, M. Venturi, *Acc. Chem. Res.* **1998**, *31*, 26–34; b) Y. Kobuke, K. Ogawa, *Bull. Chem. Soc. Jpn.* **2003**, *76*, 689–708; c) M.-S. Choi, T. Yamazaki, I. Yamazaki, T. Aida, *Angew. Chem.* **2004**, *116*, 152–160; *Angew. Chem. Int. Ed.* **2004**, *43*, 150–158; d) E. C. Constable, R. W. Handel, C. E. Housecroft, A. F. Morales, B. Ventura, L. Flamigni, F. Barigelletti, *Chem. Eur. J.* **2005**, *11*, 4024–4034.

[12] Switching of electron transfer has been achieved with a Ru/Os tetranuclear complex: M. Haga, M. M. Ali, R. Arakawa, *Angew. Chem.* **1996**, *108*, 85–87; *Angew. Chem. Int. Ed. Engl.* **1996**, *35*, 76–78.

[13] J. Otsuki, N. Omokawa, K. Yoshiba, I. Yoshikawa, T. Akasaka, T. Suenobu, T. Takido, K. Araki, S. Fukuzumi, *Inorg. Chem.* **2003**, *42*, 3057–3066.

[14] S. D. Ernst, W. Kaim, *Inorg. Chem.* **1989**, *28*, 1520–1528.

[15] P. R. Ashton, C. L. Brown, J. Cao, J.-Y. Lee, S. P. Newton, F. M. Raymo, J. F. Stoddart, A. J. P. White, D. J. Williams, *Eur. J. Org. Chem.* **2001**, 957–965.

[16] J. B. Flanagan, S. Margel, A. J. Bard, F. C. Anson, *J. Am. Chem. Soc.* **1978**, *100*, 4248–4253.

[17] a) J. L. Sadler, A. J. Bard, *J. Am. Chem. Soc.* **1968**, *90*, 1979–1989; b) A. J. Bellamy, I. S. MacKirdy, C. E. Niven, *J. Chem. Soc. Perkin Trans. 2* **1983**, 183–185.

[18] a) A. Juris, V. Balzani, F. Barigelletti, S. Campagna, P. Belser, A. Von Zelewsky, *Coord. Chem. Rev.* **1988**, *84*, 85–277; b) K. Kalyanasundaram, *Photochemistry of Polypyridine and Porphyrin Complexes*, Academic Press, London, **1992**.

[19] Several possibilities may be invoked as the reasons for the nonluminescent nature of this complex, as discussed for related azopolypyridine complexes.[3f] Briefly, the possibilities include the energy gap law, twisting about N=N double bonds, the internal conversion to the azobpy localized triplet state, and an increased basicity of the azo groups. For more detailed discussion, see ref. [3f] and references therein.

[20] N. H. Damrauer, G. Cerullo, A. Yeh, T. R. Boussie, C. V. Shank, J. K. McCusker, *Science* **1997**, *275*, 54–57.

[21] G. B. Shaw, D. J. Styers-Barnett, E. Z. Gannon, J. C. Granger, J. M. Papanikolas, *J. Phys. Chem. A* **2004**, *108*, 4998–5006.

[22] S. Welter, N. Salluce, A. Benetti, N. Rot, P. Belser, P. Sonar, A. C. Grimsdale, K. Müllen, M. Lutz, A. L. Spek, L. De Cola, *Inorg. Chem.* **2005**, *44*, 4706–4718.

[23] a) The time constants of the interligand electron transfer with the same order of magnitude have been reported for other mixed ligand complexes, such as 0.7 ps for $[Ru(phen)_2dppz]^{2+}$ (phen = 1,10-phenanthroline, dppz = dipyrido[3,2-*a*:2′-3′-*c*]phenazine) (see ref. [23b]) and 1.5 ps for a mixed ligand osmium complex (see ref. [23c]); b) B. Önfelt, P. Lincoln, B. Nordén, J. S. Baskin, A. H. Zewail, *Proc. Natl. Acad. Sci. USA* **2000**, *97*, 5708–5713; c) G. B. Shaw, C. L. Brown, J. M. Papanikolas, *J. Phys. Chem. A* **2002**, *106*, 1483–1495.

[24] C. Creutz, M. Chou, T. L. Netzel, M. Okumura, N. Sutin, *J. Am. Chem. Soc.* **1980**, *102*, 1309–1319.

[25] a) The free energy values for the MLCT states involving the bpy ligands were obtained from a spectral fitting of the emission profile at 77 K in Figure 9, using the relation: $\Delta G = E_0 + \lambda$, where E_0 is the energy gap and λ is the reorganization energy. E_0 was obtained from the emission maxima and λ is given by $\lambda = (\Delta\tilde{\nu}_{1/2})^2 (16 k_B T \ln 2)^{-1}$, where $\Delta\tilde{\nu}_{1/2}$ is the full width at half-maximum, k_B is the Boltzmann constant, and T is temperature (see ref. [25b,c]). The parameters for the fit were $E_0 = 1.91$ eV and $\Delta\tilde{\nu}_{1/2} = 0.13$ eV for $(bpy)Ru^{III}(bpy^{\bullet-})(azobpy)Os^{II}$ (1.96 eV), $E_0 = 1.88$ eV and $\Delta\tilde{\nu}_{1/2} = 0.17$ eV for $(bpy)Ru^{III}(bpy^{\bullet-})(azobpy^{\bullet-})Os^{II}$ (1.98 eV), and $E_0 = 1.68$ eV and $\Delta\tilde{\nu}_{1/2} = 0.11$ eV for $(bpy)Ru^{II}(bpy)(azobpy^{2-})Os^{III}$ (1.72 eV). The free energy for $(bpy)Ru^{III}(bpy)(azobpy^{\bullet-})Os^{II}$ was taken to be less than that for $(bpy)Ru^{III}(bpy^{\bullet-})(azobpy)Os^{II}$ by 0.57 eV on the basis of the absorption spectrum. The free energy for $(bpy)Ru^{III}(bpy)(azobpy^{2-})Os^{II}$ was just placed between those of $(bpy)Ru^{III}(bpy^{\bullet-})(azobpy^{\bullet-})Os^{II}$ and $(bpy)Ru^{II}(bpy)(azobpy^{2-})Os^{III}$; b) K. A. Opperman, S. L. Mecklenburg, T. J. Meyer, *Inorg. Chem.* **1994**, *33*, 5295–5301; c) J. A. Roberts, J. P. Kirby, D. G. Nocera, *J. Am. Chem. Soc.* **1995**, *117*, 8051–8052.

[26] A small amount of aqueous HNO_3 is added for the electrolysis to obtain reproducible spectral responses (see Experimental section). Acid may stabilize the reduced species by protonation on the azo radical anion.

[27] Substituents on the bpy rings greatly affect the luminescence quantum yields of $[Ru(bpy)_3]^{2+}$-type complexes. An amino substituent, an analogue to the reduced azo group, exerts an aggravating effect in terms of luminescence: M. J. Cook, A. P. Lewis, G. S. G. McAuliffe, V. Skarda, A. J. Thomson, J. L. Glasper, D. J. Robbins, *J. Chem. Soc. Perkin Trans. 2* **1984**, 1293–1301.

[28] The decaying curve at around $\lambda = 750$ nm, where Os luminescence dominates, showed an almost identical time profile as the Ru luminescence, which indicates that the lifetime of the Os unit is shorter than that of the Ru unit, preventing the direct evaluation of energy transfer rate from the time-course of an increasing phase of the sensitized luminescence.

[29] S. Welter, N. Salluce, P. Belser, M. Groeneveld, L. De Cola, *Coord. Chem. Rev.* **2005**, *249*, 1360–1371.

[30] C. Chiorboli, M. A. J. Rodgers, F. Scandola, *J. Am. Chem. Soc.* **2003**, *125*, 483–491.

[31] Y. Liu, A. De Nicola, O. Reiff, R. Ziessel, F. S. Schanze, *J. Phys. Chem. A* **2003**, *107*, 3476–3485.

[32] a) N. G. Connelly, W. E. Geiger, *J. Am. Chem. Soc. Chem. Rev.* **1996**, *96*, 877–910; b) W. E. Geiger, Jr., *J. Am. Chem. Soc.* **1974**, *96*, 2632–2634.

[33] M. S. Tunuli, J. H. Fendler, *J. Am. Chem. Soc.* **1981**, *103*, 2507–2513.

[34] a) S. Fukuzumi, J. Maruta, *Inorg. Chim. Acta* **1994**, *226*, 145–150; b) S. Fukuzumi, I. Nakanishi, T. Suenobu, K. M. Kadish, *J. Am. Chem. Soc.* **1999**, *121*, 3468–3474.

[35] R. A. Jones, B. D. Roney, W. H. F. Sasse, K. O. Wade, *J. Chem. Soc. B* **1967**, 106–111.

[36] C. Lee, W. Yang, R. G. Parr, *Phys. Rev. B* **1988**, *37*, 785–789.

[37] a) P. J. Hay, W. R. Wadt, *J. Chem. Phys.* **1985**, *82*, 270–283; b) W. R. Wadt, P. J. Hay, *J. Chem. Phys.* **1985**, *82*, 284–298; c) P. J. Hay, W. R. Wadt, *J. Chem. Phys.* **1985**, *82*, 299–310.

Received: October 26, 2007
Published online: January 18, 2008

